frontiers | Frontiers in Materials

TYPE Original Research
PUBLISHED 28 April 2025
DOI 10.3389/fmats.2025.1557939

OPEN ACCESS

EDITED BY
Marco Guerrini,
Istituto di Ricerche Chimiche e Biochimiche G. Ronzoni, Italy

REVIEWED BY
Edwin Alexander Yates,
University of Liverpool, United Kingdom
Fuming Zhang,
Rensselaer Polytechnic Institute, United States

*CORRESPONDENCE
Stephan Harm,
stephan.harm@donau-uni.ac.at

RECEIVED 09 January 2025
ACCEPTED 04 April 2025
PUBLISHED 28 April 2025

CITATION
Harm S, Zottl J, Schildböck C, Bauer C, Cont D and Weber V (2025) Endpoint attachment of unfractionated vs low molecular weight heparin: a comparative study on blood compatibility.
Front. Mater. 12:1557939.
doi: 10.3389/fmats.2025.1557939

Endpoint attachment of unfractionated vs low molecular weight heparin: a comparative study on blood compatibility

Stephan Harm[1]*, Jennifer Zottl[1], Claudia Schildböck[1], Christoph Bauer[2], Denisa Cont[1,3] and Viktoria Weber[1]

[1]Department for Biomedical Research, University for Continuing Education Krems, Krems an der Donau, Austria, [2]Department for Health Sciences, Medicine and Research, University for Continuing Education Krems, Krems an der Donau, Austria, [3]Department of Physiology, Pharmacology and Microbiology, Karl Landsteiner University of Health Sciences, Krems an der Donau, Austria

Introduction: Blood compatibility is a critical requirement for materials used in medical devices to prevent adverse reactions such as thrombosis and inflammation. Heparin, a natural anticoagulant, is commonly used to coat medical devices such as catheters and stents, mimicking the endothelial glycocalyx and thereby preventing thrombus formation. While endpoint attached (EPA) heparin surfaces have proven effective in clinical use, concerns have arisen regarding heparin-induced thrombocytopenia (HIT) associated with unfractionated heparin (UFH)-bonded prostheses. Given the lower HIT risk profile of low molecular weight heparin (LMWH), this study aimed to evaluate the blood compatibility of LMWH-functionalized surfaces in comparison to those functionalized with UFH.

Methods: Conventional 96-well plates and adsorbent materials were functionalized with either UFH or LMWH. The blood compatibility of these surfaces was assessed by analyzing coagulation parameters, platelet adhesion, and leukocyte adhesion. Antithrombin III (AT-III) binding was also examined to understand the anticoagulant mechanism of LMWH-functionalized surfaces.

Results: LMWH-functionalized surfaces demonstrated no significant binding to AT-III. Despite this, both LMWH- and UFH-functionalized surfaces effectively prevented the activation of coagulation triggered by foreign surfaces. Furthermore, there was no observed increase in platelet or leukocyte adhesion on LMWH-functionalized surfaces compared to UFH-functionalized ones, indicating a similar degree of blood compatibility between the two.

Discussion: This study highlights that LMWH can provide blood compatibility comparable to that of UFH when used for surface functionalization, despite its lack of AT-III binding. These findings support the potential of LMWH as a safer alternative to UFH in medical device coatings, particularly in applications where the risk of HIT must be minimized.

KEYWORDS

endpoint attached heparin, low molecular weight heparin (LMWH), unfractionated heparin (UFH), blood compatibility, heparin induce thrombocytopenia, carmeda bioactive surface

1 Introduction

It is crucial to ensure that materials used in medical interventions and treatments are compatible with human blood to prevent adverse reactions or complications, such as thrombosis. The endothelial glycocalyx emerges as a template for developing blood compatible surfaces. It consists of carbohydrate structures, proteins and glycoproteins and lines the luminal surface of endothelial cells in blood vessels. Its physiological functions include the regulation blood vessel permeability, prevention of clot formation, and interaction with activated blood cells. The endothelial glycocalyx is primarily composed of glycosaminoglycans, including heparan sulfate, chondroitin sulfate, dermatan sulfate, keratan sulfate and hyaluronic acid, which share structural similarities with heparin. Its precise composition varies depending on the tissue type and physiological conditions. To enhance blood compatibility, efforts have been made to coat medical materials with heparin, aiming to replicate the protective properties of the endothelial glycocalyx (Reitsma et al., 2007; Weinbaum et al., 2007). While pharmaceutical heparin is widely used as an anticoagulant, endogenously occurring heparin in mast cells primarily plays roles in immune regulation and inflammation rather than direct anticoagulation *in vivo* (Shute, 2023). Intravenously administered heparin inhibits clotting by increasing the activity of AT-III, an inhibitor of thrombin and factor Xa. Heparin-coated surfaces are used for medical devices such as catheters, stents, blood pumps or heart-lung machines to reduce or prevent the formation of thrombi (Biran and Pond, 2017).

Initial attempts to bind heparin to surfaces were achieved through ionic binding to quaternary ammonium compounds (Gott et al., 1963). However, ionically bound heparin is washed out upon contact with blood within hours. Covalent binding of heparin, on the other hand, may involve the active binding site of heparin, potentially leading to a significant reduction of its anticoagulant activity (Hsu, 1991). Consequently, Larm et al. developed an improved method by cleaving the heparin chain with nitrosyl cations to obtain terminal carbonyl groups (Larm et al., 1983), which were then end-point attached to an amino-functionalized polymer surface through reductive amination, maintaining the anticoagulant effect of heparin. Functionalization with EPA heparin, commercially known as CARMEDA BioActive Surface (CBAS heparin surface), has become a widely used method for coating medical devices, such as stents, blood pumps, catheters, and vascular prostheses. While the CBAS heparin surface has been successfully used in blood-contacting medical devices, several case reports have provided evidence for a causal relationship between HIT and heparin-coated prostheses (Thakur et al., 2009; Gabrielli et al., 2011; Wheatcroft et al., 2011; Warkentin, 2012; Blas et al., 2016; Biran and Pond, 2017).

HIT is an immune reaction involving heparin, platelet factor 4 (PF4), and IgG antibodies that leads to platelet activation, thrombocytopenia, and increased risk of thrombosis (Jg, 1988; Chong et al., 1989; Amiral et al., 1992). Type I HIT is a mild, non-immune condition causing a slight platelet reduction, usually within 4 days of starting the administration of heparin. It resolves on its own without the need to terminate heparin administration. Type II HIT, in contrast, is a severe immune-mediated reaction that significantly reduces platelet counts, typically appearing 5–14 days after starting heparin administration, and is often associated with thrombosis.

To reduce the risk of HIT in patients, LMWH is preferred over UFH for thrombosis prophylaxis. Numerous randomized trials and prospective studies comparing LMWH to UFH have demonstrated a significantly lower incidence of HIT with LMWH (Martel et al., 2005). The absolute risk of HIT with LMWH is approximately 0.2%, representing less than one-tenth of that associated with UFH (Martel et al., 2005). Studies have demonstrated that longer heparin molecules have a greater affinity for PF4 than shorter ones (Stringer and Gallagher, 1997), which may explain why LMWH therapy is associated with a lower risk of developing HIT (Lindhoff-Last et al., 2002).

Since LMWH is associated with a significantly lower risk of inducing HIT than UFH, the question arises as to whether LMWH is suitable to generate blood compatible surfaces. The aim of this study was to compare the blood compatibility between surfaces functionalized with LMWH and UFH. Conventional 96-well plates as well as adsorbent beads were functionalized with UFH and LMWH according to the method of Larm (Larm et al., 1983), and the blood compatibility of the resulting surfaces was compared in terms of their potential to induce coagulation and blood cell adhesion.

2 Materials and Methods

2.1 Chemicals and reagents

Triton X-100, RPMI-16404, nitrophenyl phosphate disodium salt hexahydrate, 4-nitrophenol, 2-amino-2-methyl-1-propanol, sodium hydroxide solution (NaOH), hydrochloric acid (HCl), magnesium chloride hexahydrate ($MgCl_2$ x $6H_2O$), sodium nitrite, sulfuric acid, potassium permanganate ($KMnO_4$), sodium cyanoborohydride ($NaBH_3CN$), polyethyleneimine (PEI), protamine sulfate, toluidine blue, Dulbecco's phosphate buffered saline (PBS), UFH, LMWH, lipopolysaccharide from *E. coli* (LPS), Eosin Y, phorbol-12-myristate-13-acetate (PMA) and ethanol were obtained from Merck (Darmstadt, Germany). Glutaraldehyde was purchased from Carl Roth (Karlsruhe, Germany). Physiological sodium chloride (NaCl) solution was obtained from Fresenius Kabi (Graz, Austria). PolymorphPrep was purchased from ProteoGenix (Schiltingheim, France) and *Bacteroides* Heparinase I was ordered from New England BioLabs (Frankfurt, Germany).

2.2 Adsorbent

A porous polyacrylate-based adsorbent (DALI, Fresenius Medical Care, Bad Homburg, Germany), clinically used for lipoprotein whole blood apheresis, served as a carrier for the functionalization with EPA heparin. It consists of porous carboxylated polyacrylamide beads with a particle size of 150–200 µm. Its pore size is approximately 100 nm, ensuring that plasma components can selectively interact with the inner surface, while excluding blood cells (Semak et al., 2022). The following abbreviations are used for the functionalized adsorbents: PA-COO, carboxylated polyacrylate-based adsorbent; PA-PEI, PEI-coated PA; PA-dUFH, dUFH-functionalized PA; PA-dLMWH, dLMWH-functionalized PA. Heparin Sepharose 6 Fast Flow (Cytiva, Marlborough, MA) was used as control. It is a spherical,

cross-linked agarose resin with an average particle size of 90 µm that is functionalized with heparin.

2.3 Human whole blood

Human whole blood was collected from healthy volunteers. All blood donations were approved by the Ethics Committee of the University for Continuing Education Krems (EK GZ 13/2015–2018). Written informed consent was obtained from all blood donors. All experiments were conducted in accordance with the Declaration of Helsinki of the World Medical Association. Blood samples were collected by trained personnel using Vacuette (Greiner Bio-One, Kremsmünster, Austria) safety blood collection sets. Depending on the specific test requirements, the following blood collection tubes were used: K_3EDTA, 9NC (3,2% citrate) and CAT Serum. Serum or plasma was obtained by centrifugation (10 min, 3,500 g, room temperature).

2.4 Functionalization of surfaces

To enhance the efficiency and stability of heparin immobilization, we employed a controlled depolymerization process to generate reactive aldehyde groups on the polymer ends. While native UFH and LMWH contain intrinsic reducing ends, the controlled cleavage of heparin chains ensures a higher density of terminal reactive aldehyde groups, facilitating more efficient covalent attachment. The functionalization process involved.

1) Partial depolymerization to generate additional aldehyde groups at the reducing termini, improving the reactivity of heparin for surface immobilization.
2) Schiff base formation, where aldehyde groups react with primary amino groups deposited on the PEI surface.
3) Reduction of Schiff bases to establish stable covalent bonds, ensuring long-term surface stability.
4) Orientation of heparin molecules by single-bond attachment, allowing functional interaction with circulating blood components while maintaining their anticoagulant properties.

This approach increases the reproducibility and stability of heparin functionalization, ensuring a functionally active surface that closely mimics the endothelial glycocalyx.

To functionalize multi-well suspension culture plates (CELLSTAR, Greiner Bio-One) and the PA beads with heparin, we utilized the method of Larm et al. (Larm et al., 1983) with minor adjustments to obtain end-point-attachment of heparin. The protocol involves partial degradation of heparin by acid hydrolysis, resulting in shorter polymers carrying reactive terminal aldehyde groups, enabling the immobilization on aminated surfaces.

2.4.1 Preparation of partially degraded heparin

Aliquots of 1,000 mg UFH or LMWH were dissolved in 300 mL of ice cooled water followed by addition of 10 mg of sodium nitrite. The pH was adjusted to 2.7 with HCl. After incubation at 1°C with constant stirring for 2 h, the reaction was stopped by adjusting the pH to 7.0 using NaOH. To obtain a high purity of desalted modified heparin with a molecular mass ≥3 kDa, the partially degraded unfractionated heparin (dUFH) solution was concentrated using centrifugal filters with a molecular cut-off of 3 kDa (Vivaspin20, Satorius, Goettingen, Germany) and washed three times with de-ionized water. Low molecular weight heparin (dLMWH) was desalted by dialysis (molecular cut off 0.1–0.5 kDa, Spectra/Por, VWR, Darmstadt, Germany) against de-ionized water. The partially degraded heparin solutions were lyophilized and stored at 4°C until use.

2.4.2 Anticoagulant activity of dUFH and dLMWH

The anticoagulant activity of UFH and LMWH was compared before and after modification (INNOVANCE Heparin Assay, Siemens Healthineers, Munich, Germany) on a Sysmex CA-600 device. Three freshly drawn citrated plasma samples were spiked with varying amounts of heparin (0–10 µg/mL) and incubated for 10 min at room temperature before measuring the anticoagulant activity.

2.4.3 Polymer length of dUFH and dLMWH

The methyl-2-benzothiazolinone hydrazone (MBTH) assay (Smith and Gilkerson, 1979; Gressler et al., 2019) was used to quantify N-acetylglucosamine (GlcNAc). This assay, along with a standard series of N-acetyl-galactosamine (GalNAc), allows for the quantification of the reduced end groups (aldehyde groups) of dUFH and dLMWH. Additionally, the total N-acetylglucosamine (GlcNAc) content can be quantified after complete acid hydrolysis (0.5 M HCl, 110°C, for 2 h). To confirm that these conditions were sufficient to fully degrade heparin polymers into disaccharide units, preliminary experiments were conducted using harsher hydrolysis conditions (4 M HCl, 100°C, 4 h). These experiments revealed no significant increase in GlcNAc yield compared to the milder conditions, indicating complete degradation under the applied protocol. The results of these control experiments and the protocol for the MBTH-assay are detailed in the Supplementary Material. The data were used to calculate the approximate polymer chain length of dLMWH and dUFH according to the following formula:

$$\frac{total\,GlcNAc\,content\,of\,dUFH\,or\,dLMWH\,[\mu M]}{amount\,of\,GlcNAc\,ends\,of\,dUFH\,or\,dLMWH\,[\mu M]} \times 675 \qquad (1)$$

where 675 Da represents the average molar mass of a heparin disaccharide unit, which typically contains an average of 2.7 sulfate groups and consists of N-acetylglucosamine (GlcNAc) and a uronic acid residue (Shriver et al., 2012).

2.4.4 End-point attachment of heparin on polystyrene well plates

Degraded heparin was covalently linked to the surface of polystyrene (PS) based 96- and 48-well suspension culture plates in three steps (Figure 1). Initially, the PS surface was carboxylated by incubation with 98% sulfuric acid containing 2 g/L $KMnO_4$ for 2 h at room temperature. Subsequently, wells were washed three times with phosphate buffer (2 M, pH 7.0) and rinsed twice with de-ionized water to eliminate remaining salts. The anionic PS surface was coated with polyethyleneimine (PEI, 25 kDa) by incubation with a 0.1% PEI solution (pH 9.0) for 1 h at room temperature. Wells were rinsed twice with 0.9% NaCl and de-ionized water to eliminate unbound PEI. Modified heparin was covalently coupled to PEI via a condensation reaction between the primary amino groups of PEI

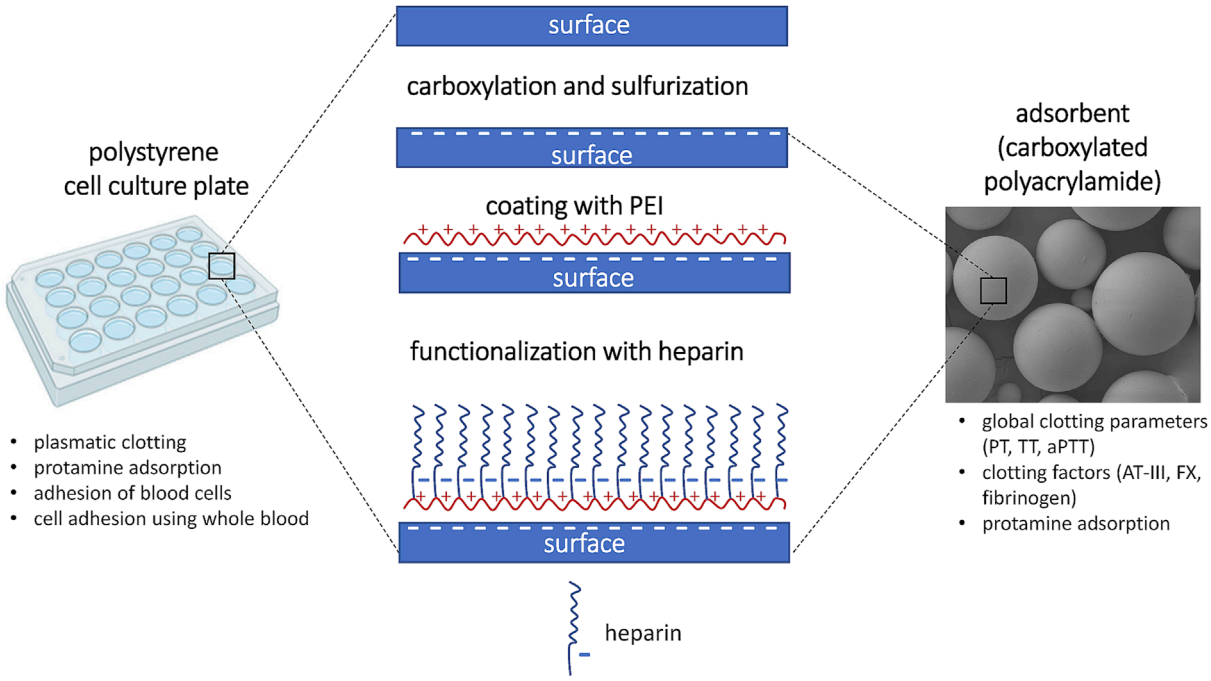

FIGURE 1
Functionalization of cell culture plates and adsorbent beads with endpoint-attached heparin.

and the terminal aldehyde groups of dUFH and dLMWH. For this purpose, modified heparin (0.2 mg/mL) was dissolved in 0.9% NaCl, and $NaBH_3CN$ (0.025 mg/mL) was added prior to pH adjustment. The pH was then adjusted to 3.5 using 1 M HCl, and the reaction mixture was incubated at 50 °C for 2 h to allow Schiff base formation and subsequent reductive amination.

While this one-step procedure follows the original protocol described by Larm et al., it is worth noting that the conventional approach to reductive amination typically involves a two-step process—initial imine (Schiff base) formation followed by reduction. Sodium cyanoborohydride is a mild reducing agent that does not directly reduce aldehydes under these conditions but selectively reduces imines once formed. Nevertheless, we acknowledge that the two-step approach may further enhance coupling efficiency and will consider this strategy in future studies. This mechanistic clarification has been added in response to reviewer feedback.

2.4.5 End-point attachment of heparin on adsorbent beads

EPA heparin functionalization of the polyacrylate-based adsorbent was performed as described for the cell culture plates (Figure 1). Since the porous adsorbent has a much larger surface area than the smooth plate, 2 mg/mL of dUFH or dLMWH and 0.025 mg/mL NaH_3BCN were used for functionalization, respectively. The ratio of adsorbent to coating solution was 1:5 (vol/vol). For washing, the functionalized adsorbent was packed into a column and rinsed with 100 mL of 0.9% NaCl per mL adsorbent at a flow rate of 1 mL/min. To remove the non-covalently bound heparin from the pores, the adsorbent was incubated in sterile de-ionized water (100 mL per mL adsorbent) for 3 weeks at room temperature, and the water was replaced daily. Finally, the adsorbent was equilibrated with 0.9% NaCl and stored at 4°C until use.

2.5 Verification of surface modification

Carboxylation and sulfation were confirmed by staining the negatively charged surface with toluidine blue, a positively charged dye. Surface amination with PEI was confirmed using Eosin Y, a negatively charged dye, yielding in a pinkish stain when bound to positively charged surfaces (Videm, 2004). To confirm heparin functionalization, a test for protamine adsorption was conducted. After incubating the coated surfaces with protamine sulfate (100 µg/mL), the protamine concentration in the supernatant was quantified by high-performance liquid chromatography (Snycerski et al., 1998) as detailed in the supplements (Supplementary Material S1).

2.5.1 Coupling density for dUFH and dLMWH

To quantify the covalently linked heparin, we enzymatically released heparin from the surface and quantified it using the MBTH assay. Aliquots of 100 µL of heparinase I (15 IU/mL, MOPS buffer, pH 7.2) were added per well and incubated at 30°C for 24 h. Acid hydrolysis was carried out as described above, followed by GlcNAc quantification using the MBTH assay. As a control, the unmodified wells were treated with the same protocol. The amount of heparin per cm^2 was determined using standard curves established with dUFH and dLMWH.

TABLE 1 Coagulation parameters and clotting factors, analyzed after incubation of fresh plasma with modified and unmodified adsorbents at a ratio of 1:10.

	Abbreviation	Measure of	Units	Reagent
Prothrombin time	PT	Extrinsic pathway of coagulation	sec	Dade innovin
Thrombin time	TT	Time for fibrin formation	sec	Test-Thrombin-Reagent
Activated partial thromboplastin time	aPTT	Intrinsic pathway of coagulation	sec	Dade Actin FS Reagent
Fibrinogen	Fib	Fibrinogen content	g/L	Dade Thrombin Reagent
Antithrombin III	AT-III	Functional activity of AT-III	% of norm	Berichrom Antithrombin III
Heparin	Hep	Heparin activity	IU/mL	INNOVANCE Heparin
Factor X	FX	Factor X activity	% of norm	Thromborel S

2.6 Influence of modified surfaces on coagulation

2.6.1 Plasmatic coagulation

EPA heparin functionalization of surfaces aims to mimic the structure of the native endothelial glycocalyx, resulting in reduced activation of coagulation via the intrinsic pathway (contact activation). The clotting time triggered by the modified surfaces PS, carboxylated PS, aminated surface (PEI) and EPA heparin (EPA dUFH or EPA dLMWH) was compared. Tests were conducted using fresh citrated plasma from three donors. Aliquots of 3 µL of 500 mM $CaCl_2$ (GESPAG Pharmacy, Bad Ischl, Austria) and 100 µL of citrated plasma were added to each well, the plate was incubated for 2 h at 37°C, and coagulation was monitored every min by recording the OD at 600 nm.

2.6.2 Clotting parameters and factors

The activated partial thromboplastin time (aPTT) serves as a screening test for defects in the intrinsic coagulation system, which includes coagulation factors V, VIII, IX and XII. A prolonged aPTT can also be caused by anticoagulants. The prothrombin time (PT) is used to assess the extrinsic pathway of plasma coagulation. PT prolongation can arise from deficiencies in coagulation factors I, II, V, X, XI, XII, and prekallikrein as well as the administration of heparin. The thrombin time (TT) focuses on the conversion of fibrinogen to fibrin. It is prolonged by heparin, thrombin inhibitors, and fibrinogen deficiency. To evaluate the effect of modified surfaces on coagulation, a batch experiment was performed with fresh human plasma utilizing the polyacrylate-based adsorbent (PA-COO^-, PA-PEI, PA-dUFH and PA-dLMWH). Commercial HepSeph was used for comparison because it differs from the EPA heparin-functionalized adsorbent in terms of how heparin is linked to the surface. Citrated blood was collected from healthy donors and the plasma was incubated at a 1:10 ratio with the adsorbents for 2 h at 37 °C with gentle agitation (n = 3). Plasma incubated without adsorbent served as control. After incubation, the plasma was analyzed to measure coagulation parameters (aPTT, PT, TT) and to quantify specific clotting factors, including fibrinogen, AT-III, and FX, using the Sysmex CA-600 instrument. All reagents (Table 1) were from Siemens Healthineers, Munich, Germany.

2.7 Blood cell adhesion on modified surfaces

To evaluate the impact of modified surfaces on blood cell adhesion, we conducted experiments with human whole blood and various blood cell fractions, including platelet-rich plasma (PRP), isolated peripheral blood mononuclear cells (PBMC), and polymorphonuclear neutrophil granulocytes (PMN). Cell adhesion was assessed indirectly by measuring the enzymatic activity and DNA (Braune et al., 2015) of adhered blood cells. Platelets were identified via acid phosphatase (ACP) (Bull et al., 2002) and lactate dehydrogenase (LDH) (Al-Samkari and Kuter, 2019). PBMCs were quantified using their DNA content (Wang and Yu, 2014) and LDH (Kumar et al., 2018). PMN adhesion was determined by neutrophil alkaline phosphatase (ALP), LDH (Kumar et al., 2018) and DNA (Sil et al., 2016). To examine surface-specific cell adhesion, we prepared 48-well cell culture plates with surfaces consisting of unmodified PS, carboxylated PS (COO^-), aminated surface (PEI) and EPA heparin-functionalized with dUFH or dLMWH (dUFH, dLMWH) and analyzed specific blood cell-markers as summarized in Tables 2, 3.

2.7.1 Platelet adhesion

PRP was obtained by centrifugation of heparinized whole blood (2 IU/mL) at 250 x g for 10 min at room temperature. To achieve a platelet concentration of 200 × 10^3/µL, PRP was diluted with platelet-poor plasma from the same donor, obtained by centrifugation at 3,500 *g* for 10 min at room temperature. PRP was incubated in the wells for 2 h at 37°C with gentle shaking (humidified atmosphere, 5% CO_2), the cell suspension was removed, and the wells were rinsed with 0.9% NaCl. Adhering cells were lysed for 30 min at 37°C using 150 µL lysis buffer (PBS containing 5 mM $MgCl_2$ and 1% Triton X-100). To quantify platelet adhesion, we determined LDH and ACP levels in the lysate, as detailed in Supplementary Material S1.

TABLE 2 Specific markers of blood cells performed after lysis of adherent blood cells.

	Abbreviation	Test
Lactate dehydrogenase	LDH	Cobas c311 analyzer with LDHI2 assay (Roche, Basel, Switzerland)
Acid phosphatase	ACP	p-Nitrophenyl phosphate Assay (Merck, Darmstadt, Germany)
Alkaline phosphatase	ALP	p-Nitrophenyl phosphate Assay (Merck, Darmstadt, Germany)
Deoxyribonucleic acid	DNA	Extraction: MagNA Pure 96 System using DNA and Viral NA SV 2.0 kit (Roche, Basel, Switzerland) Quantification: Invitrogen Quant-iT Pico Green dsDNA Assay (Thermo Fisher Scientific, Waltham, MA, United States)

TABLE 3 Analytes to detect blood cell adhesion.

	LDH	*ACP*	*ALP*	*DNA*
Whole blood	+	+	+	+
PRP	+	+	-	-
PBMC	+	-	-	+
PMN	+	-	+	+

2.7.2 Leukocyte adhesion

Leukocyte adhesion was studied using freshly separated PBMCs and PMNs, which were obtained by density centrifugation of whole blood using polymorphprep. As leukocyte adhesion is commonly accompanied by platelet activation, we combined the isolated leukocyte fractions with freshly isolated platelets from the same donor for the following cell adhesion experiments. PBMCs and PMNs were incubated at a concentration of 3×10^6 cells/µL with 200×10^3 platelet/µL in surface-modified wells for 4 h at 37°C with gentle shaking (humidified atmosphere, 5% CO_2). The cells were cultured in RPMI medium with 20% serum from the same donor. After incubation, the cell suspension was removed, and wells were rinsed with 0.9% NaCl. Adhering cells were lysed for 30 min at 37°C using 150 µL lysis buffer. PBMC adhesion was quantified via the LDH and DNA levels in the lysate. In the PMN lysate, ALP was additionally measured (Supplementary Material S1).

2.7.3 Adhesion of cells from whole blood

Freshly drawn heparinized whole blood (3 IU/mL) was activated with 10 ng/mL LPS or left untreated. Aliquots of 300 µL of activated or non-activated blood were transferred into modified 48-well plates and incubated with gentle agitation at 37°C for 4 h (humidified atmosphere, 5% CO_2). After incubation, the wells were rinsed with 0.9% NaCl and adhering cells were treated with 150 µL of lysis buffer at 37°C for 30 min. The resulting lysates were analyzed for LDH, ALP, ACP, and DNA levels as described in Supplementary Material S1.

2.7.4 Scanning electron microscopy

After incubation, washed surfaces were fixed overnight with 2.5% glutaraldehyde at 4°C. After dehydration with increasing concentrations of ethanol (10%–100%), the bottom of the wells was punched out, the discs were gold sputtered using a Q150R sputter coater (Quorum Technologies Ltd., Laughton, United Kingdom) and images were obtained on a FlexSEM 1,000 Hitachi (Mannheim, Germany).

2.8 Statistical analysis

Statistical analysis was performed using GraphPad Prism 9.3.1 (GraphPad Software, Boston, MA). The Kolmogorov-Smirnov Test was applied to check for normal distribution. Normally distributed data were compared using the t-test. For non-normally distributed data, the Mann-Whitney Rank Sum Test was used. Significances are given as follows: ns $p > 0.05$,$^{*}p \leq 0.05$,$^{**}p \leq 0.01$, and$^{***}p \leq 0.001$.

3 Results

3.1 Polymer length of dUFH and dLMWH

By quantifying the number of GlcNAc residues in the modified heparins before and after complete hydrolysis, the average polymer chain length can be calculated (Equation 1). For dLMWH, complete hydrolysis of the polymer increased the GlcNAc content by a factor of 1.9, which means that the average molecular mass of dLMWH is 1.2 kDa (two D-glucosamine and two uronic acid building blocks). For dUFH, the GlcNAc content increased by a factor of 18.4 after complete hydrolysis, resulting in an average molecular mass of 11.0 kDa. Due to its molecular mass of 5–30 kDa, unfractionated heparin molecules are partially degraded, resulting in an average of one cut per molecule. This means that the molecular mass of dUFH after chemical modification ranges between 3 and 15 kDa.

3.2 Coupling density for dUFH and dLMWH

The amount of covalently bound heparin on the modified 96-well plates was determined by enzymatic cleavage of heparin and subsequent GlcNAc quantification. While the polymer chains of dUFH are on average 10 times longer compared to dLMWH, almost equal amounts of dLMWH (4.56 ± 0.16 µg/cm^2) and dUFH (4.68 ± 0.14 µg/cm^2) were detected on the functionalized surfaces. This suggests that the coupling density of dLMWH was 10 times higher for dLMWH than for dUFH (Figure 2). To assess the stability

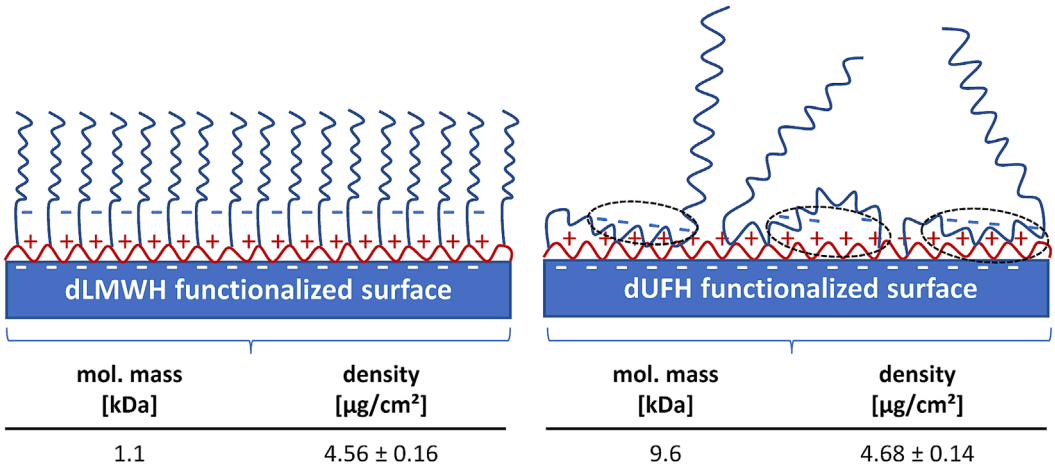

FIGURE 2
Surface functionalization with dUFH and dLMWH. The amount of bound heparin (mass per µm2) on dUFH functionalized surfaces is comparable to the amount measured on surfaces functionalized with dLMWH. The long, strongly negatively charged dUFH polymers interact with the positively charged PEI surface via ionic interactions, thereby forming a stable polyelectrolyte complex (dotted circles). Consequently, the coupling density (number of covalently linked polymers per µm2) of dUFH is lower than that of dLMWH functionalized surfaces, which are likely to possess a brush-like structure.

of endpoint attached heparin on adsorbent beads, we conducted prolonged washing experiments and monitored heparin release over several weeks. Our results indicate that >90% of immobilized heparin remained attached after 3 weeks of continuous washing, confirming high stability.

3.3 Anticoagulant properties of modified heparins

To achieve an anticoagulant activity of 1 IU/mL in plasma, 4.3 ± 0.5 µg of UFH were required, while 5.8 ± 0.5 µg were needed for dUFH. This indicates that the anticoagulant activity was only slightly reduced during the modification of UFH to dUFH. In contrast, the anticoagulant activity of dLMWH was significantly lower compared to LMWH (Figure 3). To achieve an anticoagulant activity of 1 IU/mL in plasma, 7.7 ± 0.3 µg of LMWH and 12.5 ± 1.6 µg of dLMWH were required.

3.4 Protamine binding

Protamine adsorption to heparinized surfaces confirmed the covalent binding of heparin to the PEI-functionalized surface (Figure 4). The unmodified polyacrylate-based adsorbent bound 6.11 ± 0.15 mg protamine per mL adsorbent beads. This is due to the porous nature of the adsorbent, providing a larger surface for adsorption compared to the non-porous wells. The adsorption capacity decreased to 0.63 ± 0.15 mg after PEI coating, suggesting that the porous structure was not entirely coated with PEI, leaving free carboxyl groups available. Functionalization of the PEI-coated adsorbent with heparin resulted in increased protamine adsorption (4.10 ± 0.05 mg/mL for dUFH and 1.85 ± 0.07 mg/mL for dLMWH). HepSeph, used as control, bound 5.71 ± 0.24 mg/mL of protamine.

3.5 Influence of modified surfaces on coagulation

3.5.1 Coagulation

Coagulation of plasma started 12.5 ± 2.9 min after contact with carboxylated surfaces, while coagulation was detectable after 43.8 ± 17.0 min for the uncharged PS surface and after 51.7 ± 2.9 min for the positively charged PEI-coated surface (Figure 5). No coagulation was observed for EPA heparin-functionalized surfaces.

3.5.2 Coagulation parameters and factors

Plasma treatment with PA-COO^- resulted in significantly prolonged PT and aPTT, indicating depletion of coagulation factors of the intrinsic and extrinsic systems. FX was completely depleted by the PEI-functionalized surface, inhibiting coagulation in the PT and aPTT assays. Among the adsorbents functionalized with EPA-heparin, only PA-dUFH showed a significant decrease in AT-III (−17.0% ± 1.4%) compared to the control. HepSeph depleted AT-III almost completely (−98.2% ± 1.4%), leading to a reduction of FX and a prolonged aPTT.

3.6 Blood cell adhesion to modified surfaces

3.6.1 Platelet adhesion

A comparison of the LDH and ACP levels showed that the untreated PS surface and the COO^- surface induced platelet adhesion, while no LDH and ACP activity was detected on the PEI surface and the surfaces functionalized with heparin (Figure 6A).

3.6.2 Adhesion of PBMCs

LDH and DNA levels did not differ for unstimulated and LPS-activated PBMCs (Figure 6B). The highest values, i.e., the largest

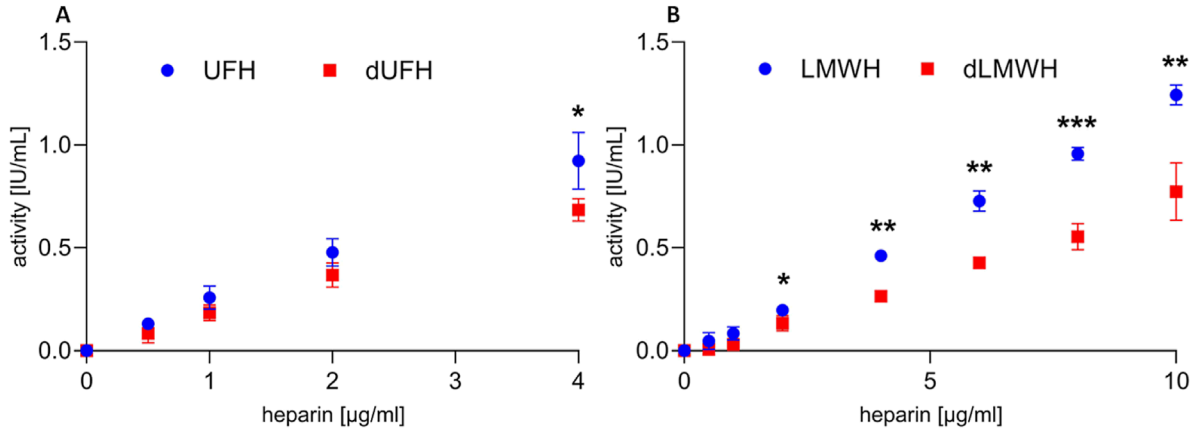

FIGURE 3
Anticoagulant activity of native and modified heparin. Freshly drawn citrate-anticoagulated plasma was spiked with unfractionated heparin **(A)** and low molecular weight heparin **(B)**, as well as the corresponding degraded heparin fractions. Data are indicated as mean ± SD (n = 3).

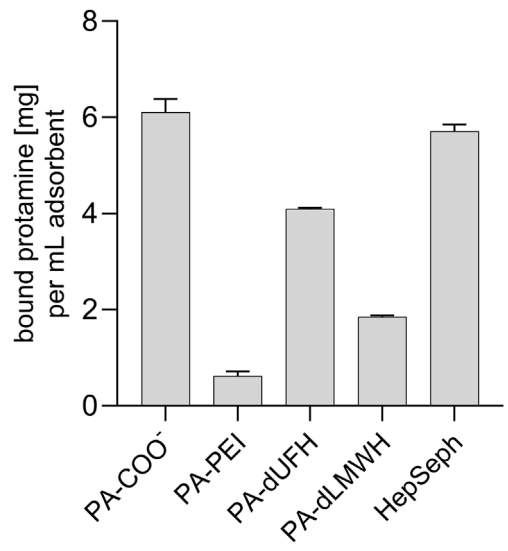

FIGURE 4
Protamine adsorption on functionalized surfaces. The protamine adsorption on unmodified and modified PA beads is shown. PA-COO-, carboxylated polyacrylate-based adsorbent; dUFH, partially degraded unfractionated heparin; dLMWH, partially degraded low molecular weight heparin; PA-PEI, PEI-coated PA; PA-dUFH, dUFH-functionalized PA; PA-dLMWH, dLMWH-functionalized PA; HepSeph, heparin Sepharose. Data are indicated as mean ± SD (n = 3).

number of adhering cells, were obtained on COO^- surfaces. The aminated PEI surface resulted in the lowest cell adhesion (lowest LDH value). It should be noted that due to the presence of LDH in platelets, this value reflects a combination of adherent PBMCs and platelets. DNA quantification indicated that the neutral PS surface also caused PBMC adhesion in addition to the COO^- modified surfaces. The surfaces functionalized with PEI, dUFH, and dLMWH demonstrated only moderate adhesion of PBMCs.

3.6.3 Adhesion of PMNs

PMN adhesion (Figure 6C) was comparable to PBMC adhesion. Surfaces functionalized with COO^- showed the highest cell adhesion, while the aminated PEI surface caused the lowest adhesion. In terms of LDH enzyme activity, cells activated with PMA exhibited higher adhesion on the PS surface than on surfaces functionalized with EPA heparin. However, as described for the experiments with PBMCs, this can be attributed to platelet adhesion. For the PMN-specific markers ALP and DNA, there was no significant difference between surfaces functionalized with dLMWH and dUFH, indicating that surfaces functionalized with longer heparin polymers do not exhibit better blood compatibility in terms of cell attachment.

3.6.4 Whole blood experiment

Surfaces functionalized with COO^- showed significantly higher numbers of adhering cells compared to other surfaces (Figure 7). Higher levels of LDH and ACP were identified for the cell lysates from the PS surface, indicating increased platelet adhesion. This was affirmed through platelet adhesion experiments. No significant difference was found in neutrophil adhesion (ALP values) among dUFH, dLMWH, PEI, and PS surfaces. However, according to DNA measurement, both, the surface functionalized with COO^- and the PS surface showed high values in LPS-stimulated whole blood, suggesting that stimulated PBMCs adhere more strongly to PS surfaces than to EPA heparin and to surfaces functionalized with PEI. No significant differences were detected between dUFH- and dLMWH-functionalized surfaces. SEM analysis confirmed the results obtained with the measurement of enzyme activities and DNA, since a higher number of cells were observed on surfaces yielding higher enzyme activities or DNA values (Figure 8).

4 Discussion

Numerous studies have reported the effectiveness of endpoint attached heparin (CBAS) for preparing blood compatible surfaces

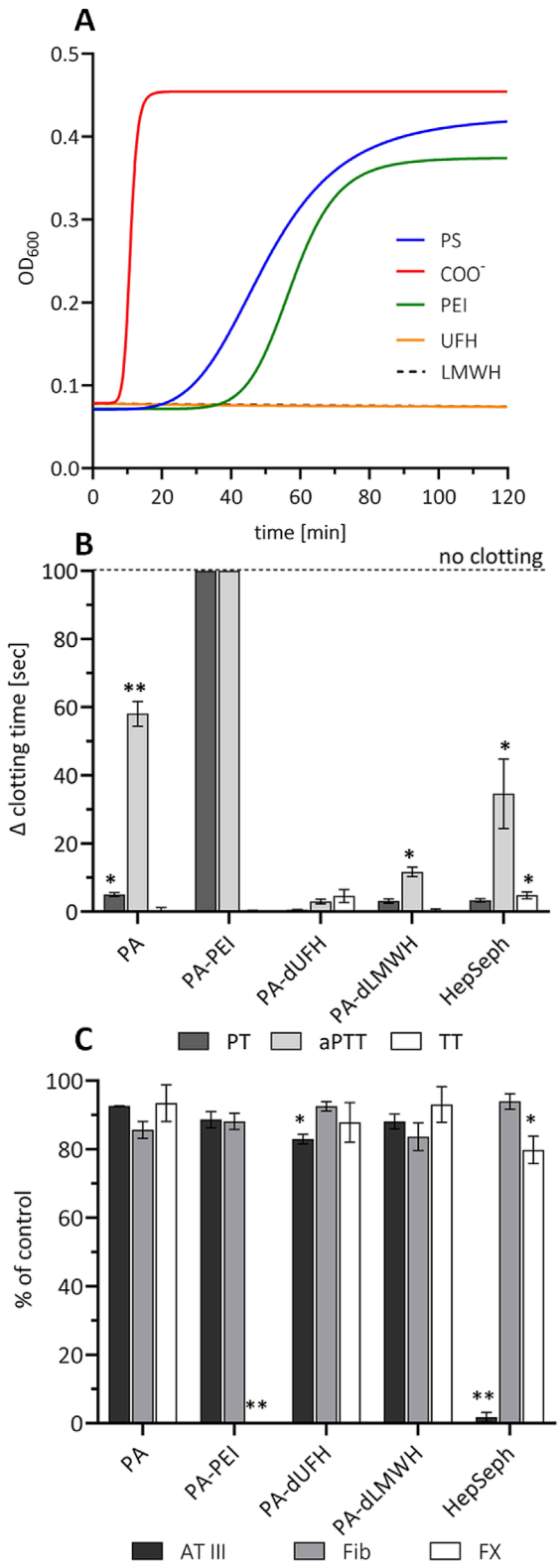

FIGURE 5
Impact of heparinized surfaces on coagulation **(A)** 96-well plates with differently modified surfaces were tested for their ability to activate coagulation, which was assessed with freshly collected plasma from four donors (OD600). The increase in the optical density is associated with fibrin formation. Global coagulation parameters PT, TT, and aPTT **(B)**, as well as AT-III, FX, and fibrinogen **(C)**, were measured. The clotting times and the values (% ± standard deviation, n = 3) compared to the control without absorbent are shown (*p > 0.05 and**p ≤ 0.05).

(Sanchez et al., 1995; Begovac et al., 2003; Jiang et al., 2010; Qiu et al., 2017). The coating of medical surfaces with heparin has a potential disadvantage, however, since heparin may cause the development of HIT. Indeed, cases of HIT observed with CBAS-coated implants have raised the question whether there was a causal connection with heparin-coated surfaces (Thakur et al., 2009; Gabrielli et al., 2011; Wheatcroft et al., 2011; Kasirajan, 2012; Warkentin, 2012; Blas et al., 2016; Biran and Pond, 2017). A possible approach to avoid heparin surface-induced HIT could be the use of LMWH instead of UFH, and we therefore compared the blood compatibility of surfaces functionalized with UFH and LMWH (Martel et al., 2005).

The average molecular mass of the modified heparins used in our study was 11.0 kDa for dUFH and 1.3 kDa for dLMWH, which corresponds to about 16 disaccharide units for dUFH and two disaccharide units for dLMWH. When comparing the anticoagulant effect of native and degraded heparins, we observed only a slight reduction of their anticoagulant effects, which was more pronounced for dLMWH. The antithrombin-binding pentasaccharide, often referred to as the AGAIA motif, contains a central glucosamine residue that is 2,3,6-trisulfated. While nitrous acid initially removes the N-sulfate group, the resulting positive amino group is stabilized by the neighboring 3-O-sulfate, which is negatively charged. This electrostatic stabilization protects the central region from further cleavage and allows the pentasaccharide sequence to resist degradation (Lindahl et al., 1984). In fact, this structural resistance is the basis for how the AGAIA motif was first identified. Consequently, it is plausible that a portion of dLMWH molecules retain functional AT-III binding sequences despite nitrous acid treatment, which would contribute to the observed anticoagulant activity.

Quantification of heparin on the functionalized surfaces revealed that similar amounts of dLMWH and dUFH (μg heparin/cm^2) were immobilized on the PS plate surface, suggesting that the coupling density (number of linked heparin molecules per cm^2) was significantly higher for dLMWH. This may be explained by the fact that the longer dUFH polymers interact with the surface through ionic interactions and thereby prevent tight functionalization through covalent coupling (Figure 2). The higher coupling density observed for dLMWH-functionalized surfaces, can be explained by additional key factors. First, smaller heparin fragments possess higher conformational mobility, allowing more effective interaction with surface-bound amino groups during coupling. Second, the chemical cleavage of heparin chains using nitrous acid produces reducing ends that are fully present in the reactive aldehyde form. In contrast, the reducing ends of native heparin or hydrolytically degraded chains are in equilibrium between cyclic (α and β) and open-chain (aldehyde) forms. The full aldehyde availability in nitrous acid-liberated sugars enhances their ability to participate in Schiff base formation and subsequent reductive amination, facilitating more efficient covalent binding.

While depletion-based quantification from the supernatant is appropriate for highly porous materials with extensive internal surface areas—such as the PA-based adsorbents used in this study—it is less suitable for flat, low-surface-area substrates like well plates, where the absolute amount of bound material is minimal. For this reason, all adsorption experiments, including protamine binding studies, were conducted using the functionalized porous adsorbents. In contrast, cell adhesion experiments were performed

10.3389/fmats.2025.1557939

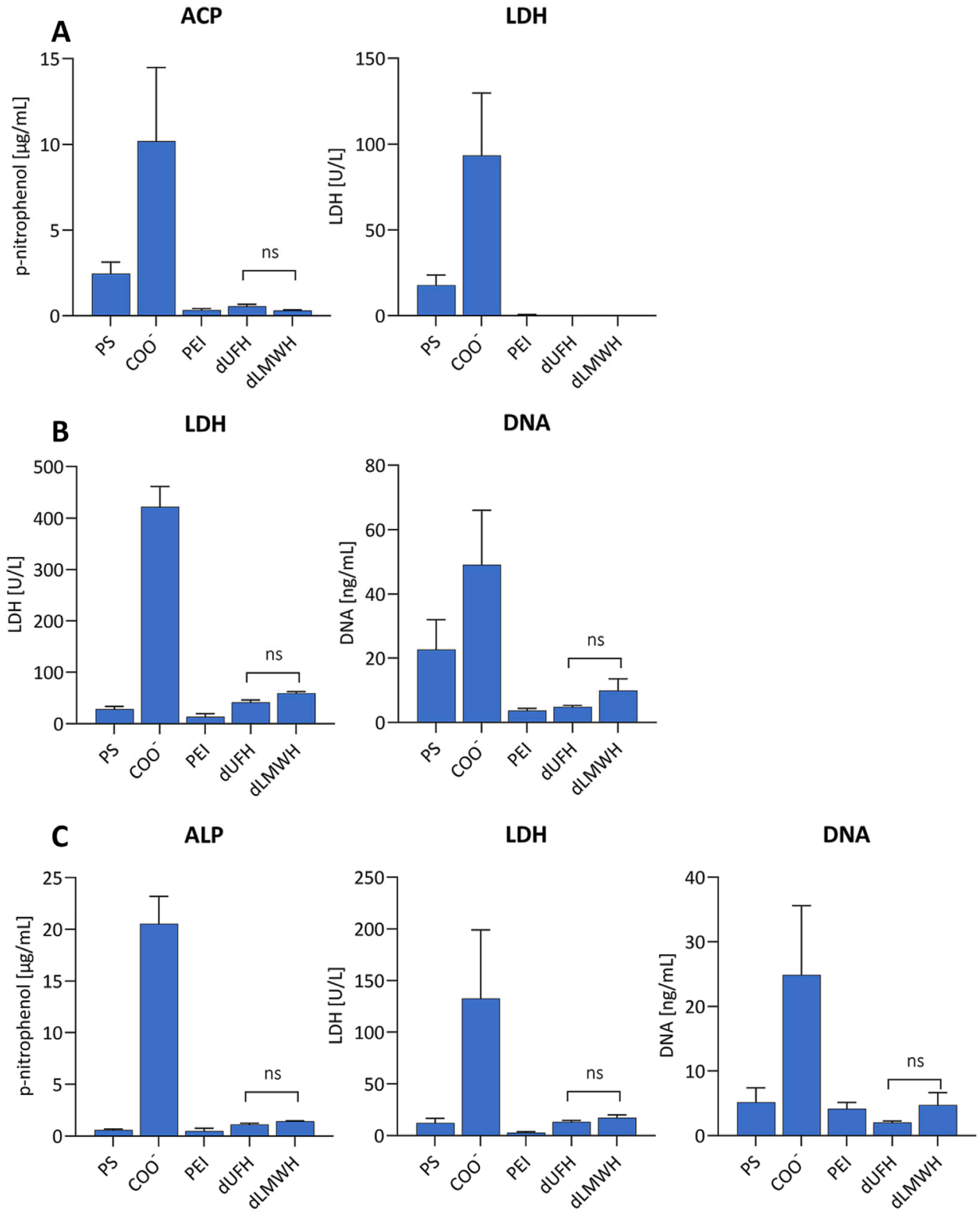

FIGURE 6
Adhesion of blood cells. Platelet-rich plasma **(A)**, peripheral blood mononuclear cells **(B)**, and polymorphonuclear leukocytes **(C)** were isolated from fresh whole blood and incubated on the modified surfaces as described in the Materials and Methods section. Cell adhesion was determined by enzyme activity (LDH, ACP, ALP) and DNA quantification in the lysates of adherent cells (n = 3).

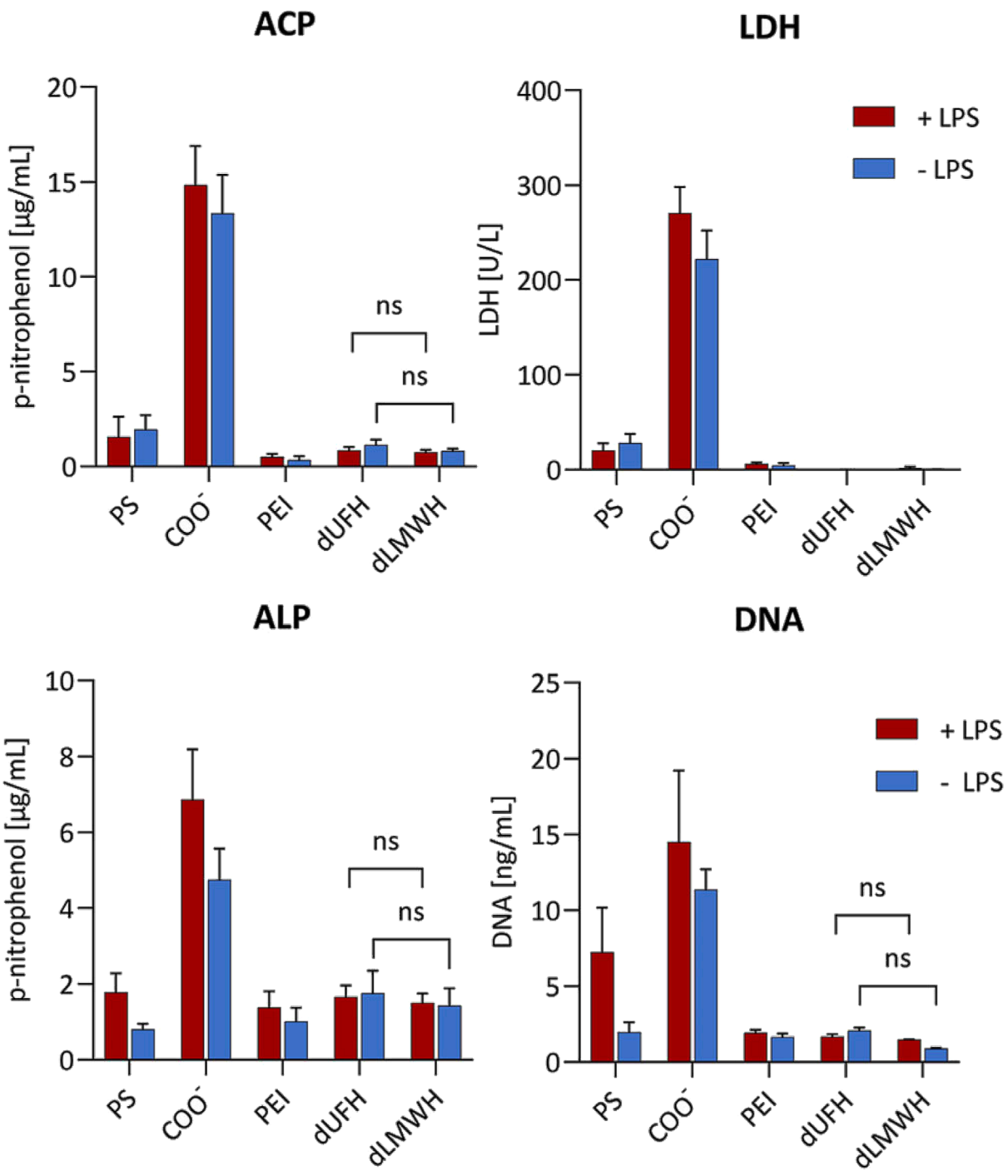

FIGURE 7
Adhesion of cells from whole blood. Whole blood was incubated on the modified surfaces. Enzymatic assays (LDH, ACP, ALP) and DNA quantification from the lysate of adherent cells were used to determine of the degree of adhesion (n = 3).

using modified 96-well plates, which provide a flat surface more suitable for microscopy and standardized adhesion assays.

Protamine binding experiments with the functionalized PA adsorbents revealed that surfaces functionalized with dUFH exhibited a significantly higher protamine adsorption capacity compared to those functionalized with dLMWH. This observation can be attributed to the longer polymer chains of dUFH, which provide multiple anionic binding sites per molecule for the polycationic protamine. In contrast, the shorter dLMWH chains offer fewer binding sites per molecule, resulting in lower overall protamine adsorption. This finding underscores the importance of polymer length in influencing the electrostatic interaction capacity of surface-bound heparin and supports the conclusion that while both dUFH and dLMWH can be effectively immobilized, their chain

10.3389/fmats.2025.1557939

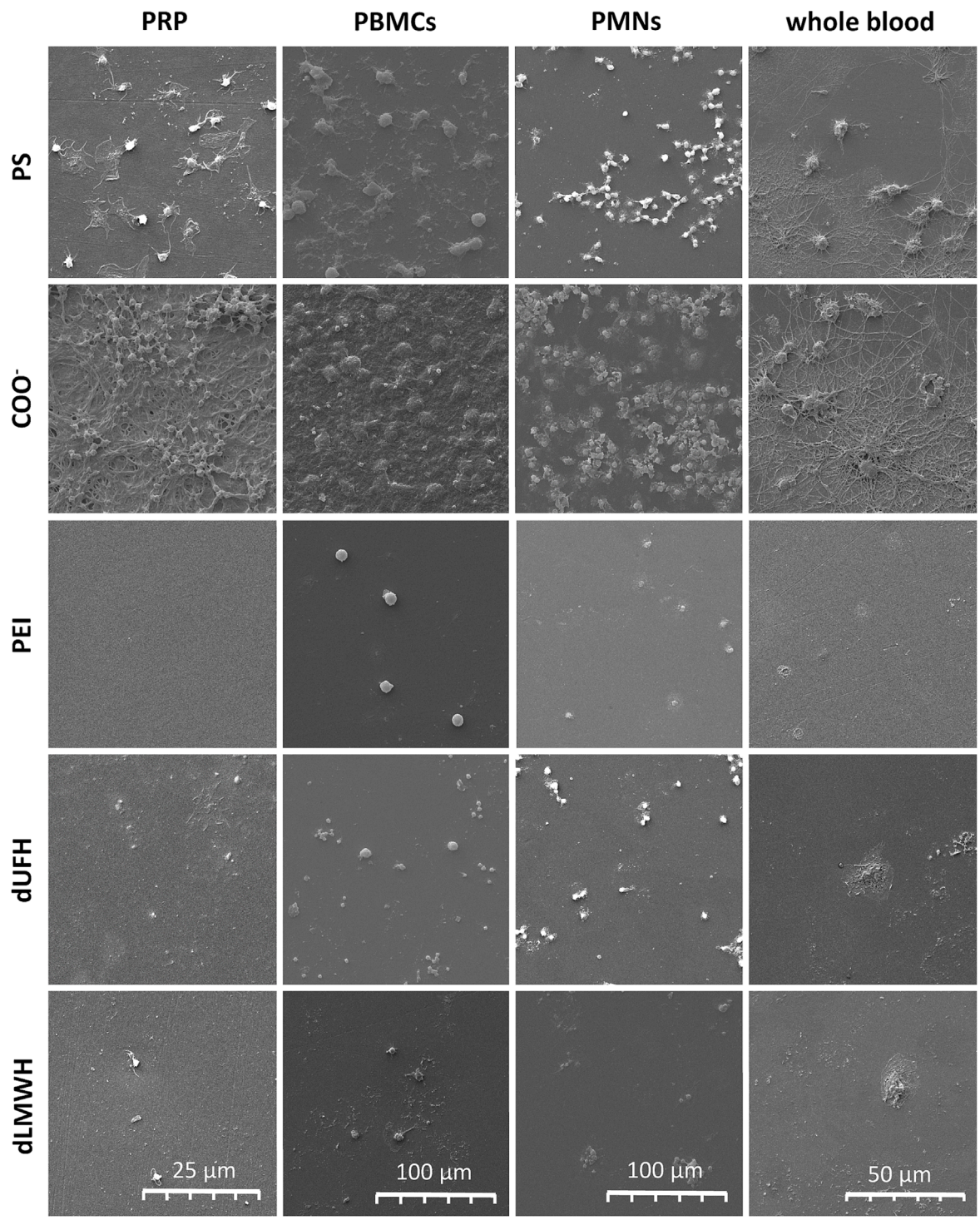

FIGURE 8
SEM images of cell adhesion. After incubation of the blood cells in the modified 96 well plates, the bottom of the plates was punched out and prepared for SEM to visualize cell.

length plays a crucial role in determining binding interactions with positively charged proteins such as protamine.

When comparing dUFH and dLMWH in terms of their impact on coagulation, only PA-dUFH demonstrated a significant reduction in AT-III levels, consistent with the fact that the thromboresistance of the CBAS surface is attributed to its AT-III binding. PA-dLMWH did not bind significant amounts of AT-III, but caused a slight prolongation of the aPTT, indicating a minor release of heparin. Our study shows that COO^- surface significantly accelerated coagulation compared to PS and the PEI-functionalized surfaces, whereas heparin-functionalized surfaces did not activate plasmatic coagulation. This indicates that EPA-functionalized surfaces with

short-chain dLMWH exhibit comparable blood compatibility as long-chain dUFH polymers. Although the average molecular weight of dLMWH is 1.3 kDa, this does not necessarily mean that all individual molecules fall below the pentasaccharide threshold required for AT-III binding. The degradation process does not completely eliminate functional pentasaccharide sequences, which typically range between 1.5 and 1.7 kDa. As a result, a fraction of dLMWH molecules likely retains the essential AT-III binding structure, thereby contributing to its anticoagulant activity. Another possible explanation for the observed anticoagulant effect is the dense functionalization of dLMWH on the surface, which may create a shielding effect that prevents the activation of the extrinsic coagulation pathway. Additionally, heparins exhibit anticoagulant activity beyond AT-III interactions. Notably, ultra-low molecular weight heparins have been shown to inhibit Factor XIIa, thereby affecting the contact activation pathway of coagulation (Pixley et al., 1991). It is likely that a combination of these mechanisms contributes to the observed anticoagulant effect, warranting further investigation into the role of pentasaccharide retention, Factor XIIa inhibition, and surface shielding in dLMWH-functionalized materials.

Next to coagulation, the activation and adhesion of blood cells to biomaterials are decisive for their blood compatibility. Particularly crucial in this process is the response of platelets. In addition to their role in thrombus formation, activated platelets interact extensively with leukocytes. By releasing chemokines, particularly chemokine ligand 5 (CCL5), and binding to leukocytes via P-selectin, platelets promote leukocyte recruitment and stimulate cytokine release. To evaluate the impact of functionalized surfaces on blood cell activation, the adhesion of cells from enriched platelet, neutrophil and PBMC fractions, as well as from whole blood was assessed. Since leukocyte adhesion is strongly influenced by activated platelets, PBMCs and PMNs were tested in the presence of platelets. The cell adhesion experiments revealed that negatively charged surfaces promote platelet adhesion, but heparin-functionalized surfaces, despite their strong negative charge, inhibit adhesion. This suggests that heparin functionalization effectively mimics the native endothelial glycocalyx in preventing platelet adhesion. Furthermore, our results provide clear evidence that surface coating with short-chain heparin polymers (dLMWH, averaging two disaccharide units) does not increase blood cell adhesion when compared to long-chain heparin polymers (dUFH, averaging 16 disaccharide units).

To the best of our knowledge, this is the first study to use LMWH for surface functionalization to develop blood-compatible surfaces. We provide evidence that, while the dLMWH-functionalized surface does not exhibit significant AT-III binding, its blood compatibility is equivalent to that of dUFH-functionalized surfaces. Previous research on the CBAS surface has demonstrated its excellent blood compatibility and, most importantly, its ability to resist thrombosis due to its affinity for AT-III. Surfaces functionalized with heparin lacking AT-III binding sites, do not exhibit good blood compatibility (Gore et al., 2014). Therefore, it is particularly noteworthy that dLMWH-functionalized surfaces, which also lack AT-III affinity, demonstrate excellent blood compatibility. The type of heparin coupling to the surface, whether endpoint-coupled or covalently multipoint-coupled, is probably decisive. For instance, heparan sulphate and chondroitin sulphate, which are the main components of the endothelial glycocalyx, exhibit low affinity to AT-III, as well, but prevent coagulation due to their brush-like arrangement on the luminal surface of blood vessels (Weitz, 2003). Therefore, the hypothesis that the reduced thrombogenicity of heparin-coated surfaces is solely triggered by its effect on AT-III is supported. The benefits of heparin coating include reduced adsorption of procoagulant and pro-inflammatory plasma proteins, as well as selective adsorption of anticoagulant and anti-inflammatory plasma proteins. This leads to the rapid formation of a blood-friendly secondary membrane on the surface and prevents further denaturation and activation of the adsorbed proteins (Silvetti et al., 2015).

In conclusion, our study provides insights into the use of LMWH for surface functionalization of medical devices, demonstrating equal blood compatibility to traditional dUFH coatings. While LMWH-functionalized surfaces lack significant AT-III binding, they effectively mimic the native endothelial glycocalyx, preventing both plasmatic coagulation and adhesion of blood cells. The findings challenge the prevailing view that reduced thrombogenicity of heparin-coated surfaces is solely due to AT-III interaction. Although this study aims to assess the potential blood compatibility of UFH and LMWH-functionalized surfaces, we did not directly evaluate PF4 binding or HIT-specific immune responses. Future studies should incorporate HIT-specific assays, such as PF4 ELISA and platelet activation tests, to confirm whether LMWH-functionalized surfaces reduce HIT risk. It is important to acknowledge that while longer intact heparin chains are commonly implicated in the formation of immunogenic complexes with PF4, chemically modified fragments, such as those generated by nitrous acid treatment, may also pose a risk. The cleavage of N-sulfated glucosamine residues produces free amino groups, which are protonated under physiological conditions and may introduce new charge patterns capable of interacting with PF4. The presence of such positively charged modifications within longer oligosaccharide fragments could potentially result in novel immunogenic epitopes. While our current study did not assess PF4 binding or immune complex formation, future investigations should include structural characterization of the modified heparins, particularly regarding residual free amines, as well as functional PF4-binding assays to fully assess the immunogenic potential of LMWH- and UFH-functionalized surfaces. Despite these promising results, further research is essential to confirm the safety and efficacy of LMWH-functionalized surfaces, particularly regarding the potential for HIT-free applications in clinical settings.

Data availability statement

The raw data supporting the conclusions of this article will be made available by the authors, without undue reservation.

Ethics statement

The studies involving humans were approved by Ethics Committee of the University for Continuing Education Krems

(EK GZ 13/2015–2018). The studies were conducted in accordance with the local legislation and institutional requirements. Written informed consent for participation in this study was provided by the participants' legal guardians/next of kin.

Author contributions

SH: Conceptualization, Data curation, Formal Analysis, Funding acquisition, Investigation, Methodology, Project administration, Visualization, Writing – original draft, Writing – review and editing. JZ: Formal Analysis, Investigation, Visualization, Writing – review and editing. CS: Conceptualization, Data curation, Formal Analysis, Investigation, Software, Validation, Visualization, Writing – original draft. CB: Methodology, Resources, Software, Validation, Writing – review and editing. DC: Data curation, Formal Analysis, Methodology, Resources, Software, Visualization, Writing – review and editing. VW: Conceptualization, Funding acquisition, Project administration, Supervision, Writing – review and editing.

Funding

The author(s) declare that financial support was received for the research and/or publication of this article. This work was funded by the Government of Lower Austria and the European Regional Development Fund (Project ID WST3-F-5030664/030-2022).

Conflict of interest

The authors declare that the research was conducted in the absence of any commercial or financial relationships that could be construed as a potential conflict of interest.

Generative AI statement

The author(s) declare that no Generative AI was used in the creation of this manuscript.

Publisher's note

Supplementary material

The Supplementary Material for this article can be found online at: https://www.frontiersin.org/articles/10.3389/fmats.2025.1557939/full#supplementary-material

References

Al-Samkari, H., and Kuter, D. J. (2019). Lactate dehydrogenase is elevated in immune thrombocytopenia and inversely correlates with platelet count. *Br. J. Haematol.* 187, e61–e64. doi:10.1111/bjh.16183

Amiral, J., Bridey, F., Dreyfus, M., Vissac, A., Fressinaud, E., Wolf, M., et al. (1992). Platelet factor 4 complexed to heparin is the target for antibodies generated in heparin-induced thrombocytopenia. *Thrombosis haemostasis* 68, 095–096. doi:10.1055/s-0038-1656329

Begovac, P., Thomson, R., Fisher, J., Hughson, A., and Gällhagen, A. (2003). Improvements in GORE-TEX® Vascular Graft performance by Carmeda® bioactive surface heparin immobilization. *Eur. J. Vasc. endovascular Surg.* 25, 432–437. doi:10.1053/ejvs.2002.1909

Biran, R., and Pond, D. (2017). Heparin coatings for improving blood compatibility of medical devices. *Adv. drug Deliv. Rev.* 112, 12–23. doi:10.1016/j.addr.2016.12.002

Blas, J.-V. V., Carsten Iii, C. G., and Gray, B. H. (2016). Heparin-induced thrombocytopenia associated with a heparin-bonded stent graft. *Ann. Vasc. Surg.* 33, 227.e1–227.e4. doi:10.1016/j.avsg.2015.11.015

Braune, S., Zhou, S., Groth, B., and Jung, F. (2015). Quantification of adherent platelets on polymer-based biomaterials. Comparison of colorimetric and microscopic assessment. *Clin. Hemorheol. Microcirc.* 61, 225–236. doi:10.3233/ch-151995

Bull, H., Murray, P. G., Thomas, D., Fraser, A. M., and Nelson, P. N. (2002). Acid phosphatases. *Mol. Pathol.* 55, 65–72. doi:10.1136/mp.55.2.65

Chong, B. H., Fawaz, I., Chesterman, C. N., and Berndt, M. C. (1989). Heparin-induced thrombocytopenia: mechanism of interaction of the heparin-dependent antibody with platelets. *Br. J. Haematol.* 73, 235–240. doi:10.1111/j.1365-2141.1989.tb00258.x

Gabrielli, R., Siani, A., Rosati, M. S., Antonelli, R., Accrocca, F., Giordano, G. A., et al. (2011). Heparin-induced thrombocytopenia type II because of heparin-coated polytetrafluoroethylene graft used to bypass. *Ann. Vasc. Surg.* 25, 840.e9–840.e12. doi:10.1016/j.avsg.2010.12.040

Gore, S., Andersson, J., Biran, R., Underwood, C., and Riesenfeld, J. (2014). Heparin surfaces: impact of immobilization chemistry on hemocompatibility and protein adsorption. *J. Biomed. Mater. Res. Part B Appl. Biomaterials* 102, 1817–1824. doi:10.1002/jbm.b.33154

Gott, V. L., Whiffen, J. D., and Dutton, R. C. (1963). Heparin bonding on colloidal graphite surfaces. *Science* 142, 1297–1298. doi:10.1126/science.142.3597.1297

Gressler, M., Heddergott, C., N'go, I. C., Renga, G., Oikonomou, V., Moretti, S., et al. (2019). Definition of the anti-inflammatory oligosaccharides derived from the galactosaminogalactan (GAG) from Aspergillus fumigatus. *Front. Cell Infect. Microbiol.* 9, 365. doi:10.3389/fcimb.2019.00365

Hsu, L.-C. (1991). Principles of heparin-coating techniques. *Perfusion* 6, 209–219. doi:10.1177/026765919100600310

Jg, K., Sheridan, D., Santos, A., Smith, J., Steeves, K., Smith, C., et al. (1988). Heparin-induced thrombocytopenia: laboratory studies. *Blood* 72, 925–930. doi:10.1182/blood.v72.3.925.925

Jiang, J.-H., Zhu, L.-P., Li, X.-L., Xu, Y.-Y., and Zhu, B.-K. (2010). Surface modification of PE porous membranes based on the strong adhesion of polydopamine and covalent immobilization of heparin. *J. Membr. Sci.* 364, 194–202. doi:10.1016/j.memsci.2010.08.017

Kasirajan, K. (2012). Outcomes after heparin-induced thrombocytopenia in patients with Propaten vascular grafts. *Ann. Vasc. Surg.* 26, 802–808. doi:10.1016/j.avsg.2011.12.011

Kumar, P., Nagarajan, A., and Uchil, P. D. (2018). Analysis of cell viability by the lactate dehydrogenase assay. *Cold Spring Harb. Protoc.* 2018, pdb.prot095497. doi:10.1101/pdb.prot095497

Larm, O., Larsson, R., and Olsson, P. (1983). A new non-thrombogenic surface prepared by selective covalent binding of heparin via a modified reducing terminal residue. *Biomater. Med. Devices Artif. Organs* 11, 161–173. doi:10.3109/10731198309118804

Lindahl, U., Thunberg, L., Bäckström, G., Riesenfeld, J., Nordling, K., and Björk, I. (1984). Extension and structural variability of the antithrombin-binding sequence in heparin. *J. Biol. Chem.* 259, 12368–12376. doi:10.1016/s0021-9258(18)90755-6

Lindhoff-Last, E., Nakov, R., Misselwitz, F., Breddin, H. K., and Bauersachs, R. (2002). Incidence and clinical relevance of heparin-induced antibodies in patients with deep vein thrombosis treated with unfractionated or low-molecular-weight heparin. *Br. J. Haematol.* 118, 1137–1142. doi:10.1046/j.1365-2141.2002.03687.x

Martel, N., Lee, J., and Wells, P. S. (2005). Risk for heparin-induced thrombocytopenia with unfractionated and low-molecular-weight heparin thromboprophylaxis: a meta-analysis. *Blood* 106, 2710–2715. doi:10.1182/blood-2005-04-1546

Pixley, R. A., Cassello, A., De La Cadena, R. A., Kaufman, N., and Colman, R. W. (1991). Effect of heparin on the activation of factor XII and the contact system in plasma. *Thromb. Haemost.* 66, 540–547. doi:10.1055/s-0038-1646456

Qiu, X., Lee, B.L.-P., Ning, X., Murthy, N., Dong, N., and Li, S. (2017). End-point immobilization of heparin on plasma-treated surface of electrospun polycarbonate-urethane vascular graft. *Acta biomater.* 51, 138–147. doi:10.1016/j.actbio.2017.01.012

Reitsma, S., Slaaf, D. W., Vink, H., Van Zandvoort, M. A., and Oude Egbrink, M. G. (2007). The endothelial glycocalyx: composition, functions, and visualization. *Pflugers Arch.* 454, 345–359. doi:10.1007/s00424-007-0212-8

Sanchez, J., Elgue, G., Riesenfeld, J., and Olsson, P. (1995). Control of contact activation on end-point immobilized heparin: the role of antithrombin and the specific antithrombin-binding sequence. *J. Biomed. Mater. Res.* 29, 655–661. doi:10.1002/jbm.820290513

Semak, V., Eichhorn, T., Weiss, R., and Weber, V. (2022). Polyzwitterionic coating of porous adsorbents for therapeutic apheresis. *J. Funct. Biomater.* 13, 216. doi:10.3390/jfb13040216

Shriver, Z., Capila, I., Venkataraman, G., and Sasisekharan, R. (2012). Heparin and heparan sulfate: analyzing structure and microheterogeneity. *Handb. Exp. Pharmacol.*, 159–176. doi:10.1007/978-3-642-23056-1_8

Shute, J. K. (2023). Heparin, low molecular weight heparin, and non-anticoagulant derivatives for the treatment of inflammatory lung disease. *Pharm. (Basel)* 16, 584. doi:10.3390/ph16040584

Sil, P., Yoo, D. G., Floyd, M., Gingerich, A., and Rada, B. (2016). High throughput measurement of extracellular DNA release and quantitative NET formation in human neutrophils *in vitro*. *J. Vis. Exp.*, 52779. doi:10.3791/52779

Silvetti, S., Koster, A., and Pappalardo, F. (2015). Do we need heparin coating for extracorporeal membrane oxygenation? New concepts and controversial positions about coating surfaces of extracorporeal circuits. *Artif. organs* 39, 176–179. doi:10.1111/aor.12335

Smith, R. L., and Gilkerson, E. (1979). Quantitation of glycosaminoglycan hexosamine using 3-methyl-2-benzothiazolone hydrazone hydrochloride. *Anal. Biochem.* 98, 478–480. doi:10.1016/0003-2697(79)90170-2

Snycerski, A., Dudkiewicz-Wilczynska, J., and Tautt, J. (1998). Determination of protamine sulphate in drug formulations using high performance liquid chromatography. *J. Pharm. Biomed. Anal.* 18, 907–910. doi:10.1016/s0731-7085(98)00285-4

Stringer, S. E., and Gallagher, J. T. (1997). Specific binding of the chemokine platelet factor 4 to heparan sulfate. *J. Biol. Chem.* 272, 20508–20514. doi:10.1074/jbc.272.33.20508

Thakur, S., Pigott, J. P., and Comerota, A. J. (2009). Heparin-induced thrombocytopenia after implantation of a heparin-bonded polytetrafluoroethylene lower extremity bypass graft: a case report and plan for management. *J. Vasc. Surg.* 49, 1037–1040. doi:10.1016/j.jvs.2008.12.004

Videm, V. (2004). Endpoint-attached heparin blocks neutrophil sticking and spreading. *Biomaterials* 25, 43–51. doi:10.1016/s0142-9612(03)00470-8

Wang, X. Y., and Yu, C. X. (2014). Research advances on DNA extraction methods from peripheral blood mononuclear cells. *Zhongguo Shi Yan Xue Ye Xue Za Zhi* 22, 1495–1498. doi:10.7534/j.issn.1009-2137.2014.05.060

Warkentin, T. E. (2012). "Heparin-coated intravascular devices and heparin-induced thrombocytopenia," in *Heparin-induced thrombocytopenia* (London: CRC Press), 585–602.

Weinbaum, S., Tarbell, J. M., and Damiano, E. R. (2007). The structure and function of the endothelial glycocalyx layer. *Annu. Rev. Biomed. Eng.* 9, 121–167. doi:10.1146/annurev.bioeng.9.060906.151959

Weitz, J. I. (2003). Heparan sulfate: antithrombotic or not? *J. Clin. investigation* 111, 952–954. doi:10.1172/jci18234

Wheatcroft, M., Greco, E., Tse, L., and Roche-Nagle, G. (2011). Heparin-induced thrombocytopenia in the presence of a heparin-bonded bypass graft. *Vascular* 19, 338–341. doi:10.1258/vasc.2011.cr0280